




Glassy heat capacity from overdamped phasons and hypothetical phason-induced superconductivity in incommensurate structures

Cunyuan Jiang ^{1,2,3}, Alessio Zaccone ⁴, Chandan Setty,⁵ and Matteo Baggioli ^{1,2,3,*}

¹*School of Physics and Astronomy, Shanghai Jiao Tong University, Shanghai 200240, China*

²*Wilczek Quantum Center, School of Physics and Astronomy, Shanghai Jiao Tong University, Shanghai 200240, China*

³*Shanghai Research Center for Quantum Sciences, Shanghai 201315, China*

⁴*Department of Physics “A. Pontremoli,” University of Milan, via Celoria 16, 20133 Milan, Italy*

⁵*Department of Physics and Astronomy, Rice Center for Quantum Materials, Rice University, Houston, Texas 77005, USA*



(Received 15 May 2023; accepted 12 July 2023; published 9 August 2023)

Phasons are collective low-energy modes that appear in disparate condensed matter systems such as quasicrystals, incommensurate structures, fluctuating charge density waves, and moiré superlattices. They share several similarities with acoustic phonon modes, but they are not protected by any exact translational symmetry. As a consequence, they are subject to a wave-vector-independent damping, and they develop a finite pinning frequency, which destroy their acoustic linearly propagating dispersion. Under a few simple, well-motivated assumptions, we compute the phason density of states, and we derive the phason heat capacity as a function of the temperature. Finally, imagining a hypothetical s -wave pairing channel with electrons, we compute the critical temperature T_c of the corresponding superconducting state as a function of phason damping using the Eliashberg formalism. We find that for large phason damping, the heat capacity is linear in temperature, showing a distinctive glasslike behavior. Additionally, we observe that the phason damping can strongly enhance the effective Eliashberg coupling, and we reveal a sharp nonmonotonic dependence of the superconducting temperature T_c on the phason damping, with a maximum located at the underdamped-to-overdamped-crossover scale. Our simple computations confirm the potential role of overdamped modes not only in explaining the glassy properties of incommensurate structures but also in possibly inducing strongly coupled superconductivity therein and enhancing the corresponding T_c .

DOI: [10.1103/PhysRevB.108.054203](https://doi.org/10.1103/PhysRevB.108.054203)

I. INTRODUCTION

Acoustic phonons are collective vibrational modes which appear in crystalline solids because of the spontaneous breaking of translations (long-range order) [1]. As Goldstone modes [2], their dispersion relation is protected by symmetries; hence phonons [3] are always gapless modes. Their dispersion relation can be obtained by solving the following equation:

$$\omega^2 = c^2 k^2 - i\omega D k^2 + \dots, \quad (1)$$

where ω and k are the frequency and wave vector, respectively, and “ \dots ” indicates higher-order terms. Here, for simplicity, we have assumed isotropy and neglected any distinction between the different branches (longitudinal or transverse). In the above equation, c and D are the phonon speed and the phonon attenuation constant. Equation (1) can be derived using several methods; see, for example, Refs. [1,4].

Many of the low-energy vibrational and thermodynamic properties of solids (e.g., density of states, heat capacity, etc.) can be efficiently rationalized starting from the simple concept of phonons, within the celebrated Debye’s theory [5]. In metallic systems, further properties, such as the electric resistivity or the onset of superconductivity, are determined,

or at least strongly affected, by phonons and their coupling to electrons. Typical cases are given by the dominant phonon-electron scattering at high temperature [6], which gives a linear-in- T resistivity above the Debye’s temperature, or the phonon-electron coupling which is behind the Bardeen-Cooper-Schrieffer (BCS) theory of superconductivity [7].

Aperiodic crystals are complex structures which do not display full translational order as in periodic crystalline structures but still enjoy long-range order; hence they are solid. Typical examples of that sort are quasicrystals, incommensurate structures, fluctuating charge density waves, and moiré superlattices. In all these different scenarios, in addition to the standard acoustic phonons, extra low-energy modes appear (e.g., Refs. [8–13]). Depending on the context, these modes are usually referred to as sliding modes or phasons. For simplicity, we will refer to them with the collective label “phason.” Despite some similarities, phasons are very different from standard acoustic phonons, and many of their peculiar properties follow from these differences. In composite crystals, or incommensurate charge density wave systems, these modes correspond to the relative rigid translations of the two superstructures along the incommensurate direction, see Fig. 1. In modulate structures, the phason, as the name indicates, it is just the fluctuation of the phase of the static modulation wave. In quasicrystals, the phason corresponds to translations in the direction perpendicular to the irrational cut

*b.matteo@sjtu.edu.cn

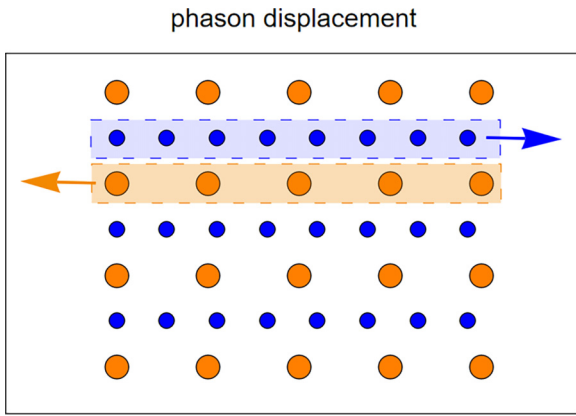


FIG. 1. A visualization of the phason displacement in an incommensurate structure with two incommensurate lattices. A concrete example is that of the mercury chain compound $\text{Hg}_{3-\delta}\text{AsF}_6$ [19,20]. The phason corresponds to a relative rigid translation between the two lattices.

in the extradimensional superspace picture [14,15], and it is harder to visualize (and indeed its meaning is still controversial [16]). See Ref. [17] for a nice review about excitations in incommensurate phases of various types. Notice that in many situations (for example, in quasicrystals), phasons do not correspond to the translations of atoms but rather to particle rearrangements, more *akin* to the diffusive motion in liquids (see, for example, Ref. [18]).

Importantly, no matter the specific microscopic structure from which they arise, phasons do not correspond to an exact translational symmetry, and therefore, differently from acoustic phonons, they are not protected by symmetry. In mathematical terms, this implies that their dispersion relation follows from an equation of the form

$$\omega^2 - \Omega(k)^2 + i\omega\Gamma(k) = 0, \quad (2)$$

where $\Omega(k)$ and $\Gamma(k)$ are not constrained to vanish in the limit of $k \rightarrow 0$. In other words, the phason dispersion relation can be characterized by a pinning frequency ω_0 and a friction or damping term γ , given by

$$\Gamma(0) \equiv \gamma, \quad \Omega(0) \equiv \omega_0. \quad (3)$$

Both terms are not allowed for acoustic phonons. For a discussion about the pinning frequency in charge density waves, see, for example, Ref. [21]. Interestingly, for pseudo-Goldstone modes, the two parameters above, ω_0 and γ , are indeed related [4] in a way similar to the famous Gell-Mann–Oakes–Renner relation for pions.

In the limit of weak quenched disorder, or equivalently large anharmonic interactions and dissipation, the pinning frequency term can be neglected, since $\omega_0 \ll \gamma$ (see Ref. [22] for an estimate in twisted bilayer graphene). Hence the dispersion relation for the phason can be well approximated by solving the following equation:

$$\omega^2 + i\omega\gamma = v^2k^2, \quad (4)$$

where v and γ are the phason speed and friction, respectively (see the next section for more details). This structure can be derived in several ways, from hydrodynamics [23] and vibrational models [24] to arguments based purely on

symmetries and effective field theory [25]. Interestingly, the dispersion which arises from solving the above equation is identical to that expected for shear waves in liquids [26] and, in general, for systems described by quasihydrodynamics [27]. In particular, there appears a crossover between an overdamped regime and an underdamped propagating one by decreasing the wavelength [24,28–31]. Both the overdamped behavior and the underdamped behavior have been experimentally observed using inelastic neutron-scattering experiments in biphenyl [32] and light-scattering experiments in BaMnF_4 [33].

Aside from their peculiar dispersion, phason modes have been identified as the fundamental origin for the glassylike properties of incommensurate structures and aperiodic crystals, which have been revealed in several instances in the literature [34–36]. More precisely, the phason gap, ω_0 , has been shown to give an excess in the heat capacity *akin* to that observed in glasses, also known as the boson peak [37]. The role of the pinned phason is similar in spirit to the possible contributions from soft optical modes [38,39], which are evident in thermoelectrics [40] and organic compounds [41,42]. There is clear evidence of the role of the phason gap in this regard [35,36,43].

On top of that, the overdamped nature of phasons for low wave vectors has been shown to produce a linear-in- T contribution to the heat capacity, similar to that of two-level states (TLSs) in glasses [35,36,43–45]. A quasilinear scaling of the heat capacity has indeed been observed in several incommensurate compounds [43,46,47]. Let us also emphasize the similarity between phasons in incommensurate structures and vortons in superconducting vortex lattices [48]. Both excitations are acousticlike bosonic modes which appear overdamped for large wavelengths. Not coincidentally, a linear-in- T heat capacity in superconducting vortex lattices has been already found and attributed to the vorton contribution [49–51]. We expect the features described in this paper, and related literature, to be generic in the presence of overdamped acousticlike modes. Interestingly, further relations between the physics of incommensurate orders (and specially pinned fluctuating charge density waves) and that of glasses have been discovered in the past [52,53]. We will return to this connection and to the possible universal relation to overdamped dynamics in Sec. VI.

Less investigated features of phasons are their coupling to electrons and their role in electronic transport, and, finally, their role in possible superconducting instabilities. This topic has been recently revived by the growing interest around twisted bilayer graphene (TBG), in which a phason mode is expected as a result of the rotational degree of freedom between the two layers [22,54–56]. The role and strength of electron-phason coupling have been recently investigated in Refs. [22,57], and the effects of phason-electron scattering have been investigated in Ref. [58].

Given its overdamped nature, the phason is expected to originate additional spectral weight at very low energy which can potentially enhance the effective coupling to electrons and therefore superconductivity. This effect might appear as general in incommensurate structures, and it has been already reported experimentally in a quasiperiodic host-guest structure of elemental bismuth at high pressure, Bi-III [59].

The superconductivity enhancement induced by incommensurability has also been recently advocated in the weak and intermediate coupling regimes in Ref. [60]. The role of gapped phasons has been also investigated in incommensurate host-guest phases in compressed elemental sulfur in Ref. [61]. More generally, the application of high pressure can transform a single-element metal into an incommensurate guest-host structure, as for the case of scandium [62]. Pressure can therefore be used as an external dialing parameter to adjust and control commensurability, and therefore the properties of the corresponding phason, providing a big potential to gauge superconductivity. Additionally, phasons could play a fundamental role not only in the recently discovered superconductivity of quasicrystals [63] but also in cuprate oxide high-critical-temperature (high- T_c) superconductors, where fluctuating charge density wave order exists in the vicinity of the superconducting phase (e.g., Refs. [64–66]), and it might be responsible for several of the mysterious properties therein [67–71].

Finally, the mechanical properties of incommensurate structures and their relation to phason dynamics are also the subject of intense investigation (e.g., Refs. [72–75]).

All in all, the motivations to study the effects of phasons on the mechanical, thermodynamic, transport, and superconducting properties of incommensurate systems are many and timely. Following the Occam’s razor principle, we present a concrete analysis in this direction based on a few simple assumptions. First, we take the limit in which the phason pinning frequency is subleading with respect to the phason damping γ . Then, we assume an s -wave isotropic pairing channel between phasons and electrons, as for the case of phonons.

In this paper, we confirm the role of overdamped propagating modes for the glasslike properties of incommensurate structures at low temperature. Most importantly, we show using the Eliashberg formalism that overdamped phasons could lead to strongly coupled superconductivity and that their damping enhances the critical temperature T_c in the underdamped case. Our findings are in agreement with the experimental results of Ref. [59] and the recent theoretical analysis in Ref. [60]. Also, the overdamped nature of the phason modes is ultimately due to anharmonicity, and it constitutes another interesting case for the sometimes fundamental role of the latter for superconductivity (see Ref. [76] for a review).

II. PHASON MODES

We start by considering the phason Green’s function given by

$$G(\omega, k) = \frac{1}{-\omega^2 + v^2k^2 - i\omega\gamma}, \quad (5)$$

where ω and k are the phason frequency and wave vector, respectively. Additionally, v and γ are the phason velocity and the friction or damping parameter, respectively. The latter can be identified with the inverse relaxation time $\gamma \equiv \tau^{-1}$. Here, we have assumed that the pinning frequency ω_0 of the phason, induced by disorder or impurities, is negligible. In other words, we assume $\gamma \gg \omega_0$. Notice that the phason

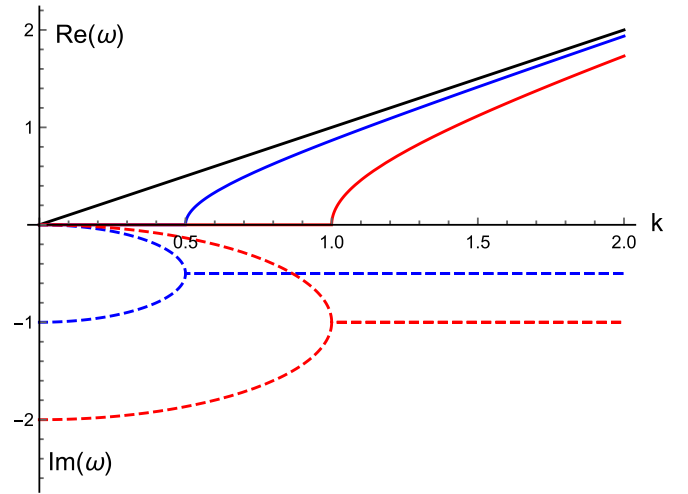


FIG. 2. Phason dispersion relation upon increasing the friction parameter γ and keeping the phason speed fixed. In this plot, $v = 1$; $\gamma = 10^{-3}$, 1, and 2 for black, blue, and red, respectively. Solid and dashed lines are the real and imaginary parts, respectively, of the dispersion relation $\omega(k)$ in Eq. (6).

dispersion relation obtained from Eq. (5) is fundamentally different from the dispersion of acoustic and optical phonons. Acoustic phonons cannot display a wave-vector-independent damping term since their dispersion is protected by translational symmetry. Also, optical phonons have a non-negligible ω_0 which, at least in the most common case of underdamped optical modes, is much larger than the friction term γ . This can be partially understood by the fact that ω_0 for phasons arises from explicitly breaking the emergent “sliding” symmetry (see, for example, Ref. [25]), while for optical phonons that is not the case as ω_0 is simply a manifestation of nonuniversal microscopic physics. As a direct consequence, ω_0 cannot be tuned to zero in the case of optical phonons, while it can in the case of phasons just assuming the absence of disorder and/or impurities. Following this assumption, the dispersion relation of the phason mode is given by

$$\omega = -\frac{i\gamma}{2} \pm \sqrt{v^2k^2 - \frac{\gamma^2}{4}}. \quad (6)$$

The real and imaginary parts of the dispersion are shown in Fig. 2. In the long-wavelength limit, or equivalently for small wave vectors, the phason is an overdamped mode with diffusive dispersion,

$$\omega = -iD_\gamma k^2 + \dots, \quad D_\gamma = v^2/\gamma, \quad (7)$$

and a second nonhydrodynamic damped mode, $\omega = -i\gamma$, appears as well. We can then identify a crossover between the overdamped regime at low k and an underdamped one at large k , in which the phason mode is propagating with a dispersion:

$$\omega = \pm vk - \frac{i\gamma}{2} + \dots. \quad (8)$$

In such a regime, $\text{Re}(\omega) \gg \text{Im}(\omega)$. More precisely, by equating the real and imaginary parts of the dispersion, Eq. (6), we

can find the crossover wave vector, which turns out to be

$$k^* = \frac{\gamma}{\sqrt{2}v}, \quad (9)$$

or equivalently,

$$\omega^* = \frac{\gamma}{2}. \quad (10)$$

Notice how this criterion, up to the $\sqrt{2}$ factor, reduces to the more familiar collisionless limit $\omega\tau \gg 1$.

Additionally, let us notice how the real part develops only after a certain critical wave vector:

$$\bar{k} = \frac{\gamma}{2v}, \quad (11)$$

which is smaller than the crossover scale. In other words, for $\bar{k} < k < k^*$, the phason dispersion has a finite real part, but the phason is still a nonpropagating overdamped mode. As explained above, for small values of γ the dynamics is underdamped, $\text{Re}(\omega) \gg \text{Im}(\omega)$. This situation is reversed for large values of the damping γ . In order to better qualify the strength of the damping γ , we introduce the frequency scale $\omega_D = vk_D$, where ω_D and k_D are the maximum frequency and wave vector, respectively, in the system—the Debye scale. The latter will explicitly enter into the definition of the phason density of states in the next section, Eq. (13). We can then define a dimensionless damping $\tilde{\gamma} \equiv \gamma/\omega_D$. With these notations, the weak damping regime, equivalent to the underdamped dynamics, is given by the condition $\tilde{\gamma} \ll 1$, while the overdamped regime is given by the opposite limit. For simplicity, we will fix, in the rest of this paper, $\omega_D = k_D = 1$ such that numerically $\tilde{\gamma} = \gamma$ apart from their dimensions. From the Green's function in Eq. (5), it is straightforward to derive the corresponding spectral function, which reads

$$\begin{aligned} S(\omega, k) &\equiv \lim_{\epsilon \rightarrow 0} \left[-\frac{1}{\pi} \text{Im} \mathcal{G}(\omega + i\epsilon, k) \right] \\ &= \frac{1}{\pi} \frac{\gamma\omega}{(\omega^2 - v^2k^2)^2 + \gamma^2\omega^2}, \end{aligned} \quad (12)$$

and it is shown in Fig. 3 for two different values of the phason damping. For small $\tilde{\gamma}$, in the underdamped regime, we see the typical feature of a propagating sound wave. In contrast, for $\tilde{\gamma} \sim O(1)$, we observe an incoherent response characterized by a flat and smoothed-out spectrum. Notice that at this point the spectral function in Eq. (12) is not normalized. For the discussion of the density of states and the heat capacity this is irrelevant, since we will be only interested in the low-energy scaling. Nevertheless, for the study of superconductivity, that is important. Therefore we will later normalize it to compute the Eliashberg function.

III. DENSITY OF STATES

From the spectral function, Eq. (12), we can derive the phason density of states using

$$g(\omega) \equiv \frac{2\omega}{k_D^3} \int_0^{k_D} S(\omega, k) k^2 dk, \quad (13)$$

where k_D is taken to be the Debye cutoff, or in other words the maximum wave vector allowed. Here, and in the rest of

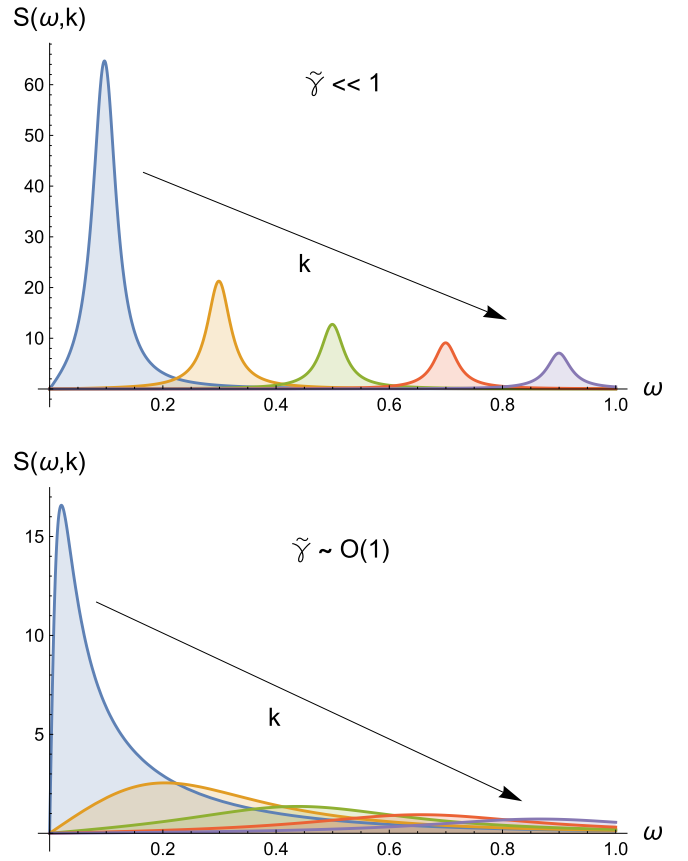


FIG. 3. Phason spectral function, Eq. (12), for small and large damping $\tilde{\gamma}$. The phason speed is fixed to $v = 1$. The top panel refers to $\tilde{\gamma} = 0.01$, while the bottom one refers to $\tilde{\gamma} = 0.5$. The wave vectors from left to right are $k = 0.1, 0.3, 0.5, 0.7$, and 0.9 , respectively.

this paper, we only consider the case of a three-dimensional system.

For small values of the damping, $\tilde{\gamma} \ll 1$, and at small frequency, we recover Debye's law

$$g(\omega) \approx \frac{\omega^2}{\omega_D^3} \equiv g_D(\omega) \quad \text{for } \tilde{\gamma} \ll 1, \quad (14)$$

where $\omega_D = k_D v$ is the Debye frequency that serves as an ultraviolet cutoff for the phason frequency. This result is certainly not surprising since in the limit of small damping the phason is a soundlike propagating acoustic wave $\omega = \pm k$, as standard acoustic phonons. Therefore, in such a limit, it just plays the role of an extra acoustic wave obeying Debye's law.

When the damping becomes a non-negligible number, $\tilde{\gamma} \sim O(1)$, the low-frequency scaling is modified to

$$g(\omega) \approx \frac{\sqrt{\tilde{\gamma}} \omega^{3/2}}{\sqrt{2} \omega_D^3} \quad \text{for } \tilde{\gamma} \sim O(1), \quad (15)$$

which can be rewritten as

$$g(\omega) = \frac{\sqrt{\omega^*} \omega^{3/2}}{\omega_D^3}. \quad (16)$$

In other words, the Debye scaling is modified as $\omega^2 \rightarrow \sqrt{\omega^*} \omega^{3/2}$. This also illustrates that the onset of this second

regime is equivalent to the condition $\omega^* > \omega$, which becomes more and more evident when $\tilde{\gamma}$ becomes large. In the limit of very large $\tilde{\gamma}$, the $\omega^{3/2}$ regime is relegated to very low frequencies, and a plateau emerges with value

$$g(\omega) \approx \frac{2}{3\pi\gamma} \quad \text{for } \tilde{\gamma} \gg 1. \quad (17)$$

A constant density of states in three dimensions is exactly what one expects from a diffusive dynamics (compare classical liquids, in which $g(0)$ is proportional to the diffusion constant [77]). In the limit of large $\tilde{\gamma}$, the second damped mode $\omega = -i\gamma$ which appears from Eq. (5) is highly damped and therefore negligible. The only low-energy mode left is the diffusive phason, with diffusion constant D_γ , Eq. (7). Using the expression for the phason diffusion constant, the value of the plateau in the density of states can be rewritten as

$$g(\omega) \sim \frac{D_\gamma}{v^2} \quad \text{for } \tilde{\gamma} \gg 1, \quad (18)$$

which is exactly of the same form as the diffusive component in liquids, where the diffusion constant there is related to self-diffusion [77].

In summary, the phason density of states interpolates between the Debye expression for solids and the diffusive result for liquids by increasing the damping γ . All of these three different regimes are shown in Fig. 4, where the dashed lines emphasize the different scalings discussed above.

IV. HEAT CAPACITY

In order to proceed with the computation of the phason heat capacity, we assume a Bose-Einstein distribution for the phason modes and compute their contribution to the heat capacity by integrating the density of states (DOS)

$$C(T) = c_1 k_B \int_0^\infty \left(\frac{\omega}{2k_B T} \right)^2 \sinh \left(\frac{\omega}{2k_B T} \right)^{-2} g(\omega) d\omega. \quad (19)$$

Here, c_1 is a normalization factor which will not play any important role in our analysis and will be fixed to 1 in the rest of this paper.

In the limit of small damping, we recover Debye's law

$$C(T) \propto T^3 \quad \text{for } \tilde{\gamma} \ll 1, \quad (20)$$

which is just a consequence of the Debye-like density of states of the underdamped phasons. For non-negligible values of the damping, we obtain a slower-than-Debye scaling law

$$C(T) \propto \sqrt{\tilde{\gamma}} T^{5/2} \quad \text{for } \tilde{\gamma} \sim O(1). \quad (21)$$

In the limit of extremely large damping, the previous scaling is pushed to very small temperature, and the heat capacity becomes approximately linear

$$C(T) \propto \frac{T}{\gamma} \propto D_\gamma T \quad \text{for } \tilde{\gamma} \gg 1. \quad (22)$$

Notice how the damping dependence here is different from the results of Ref. [35]. There, a finite pinning frequency has been assumed, and the limit of $\omega_0 \rightarrow 0$ cannot be directly taken. It would be interesting to understand this difference in more detail.

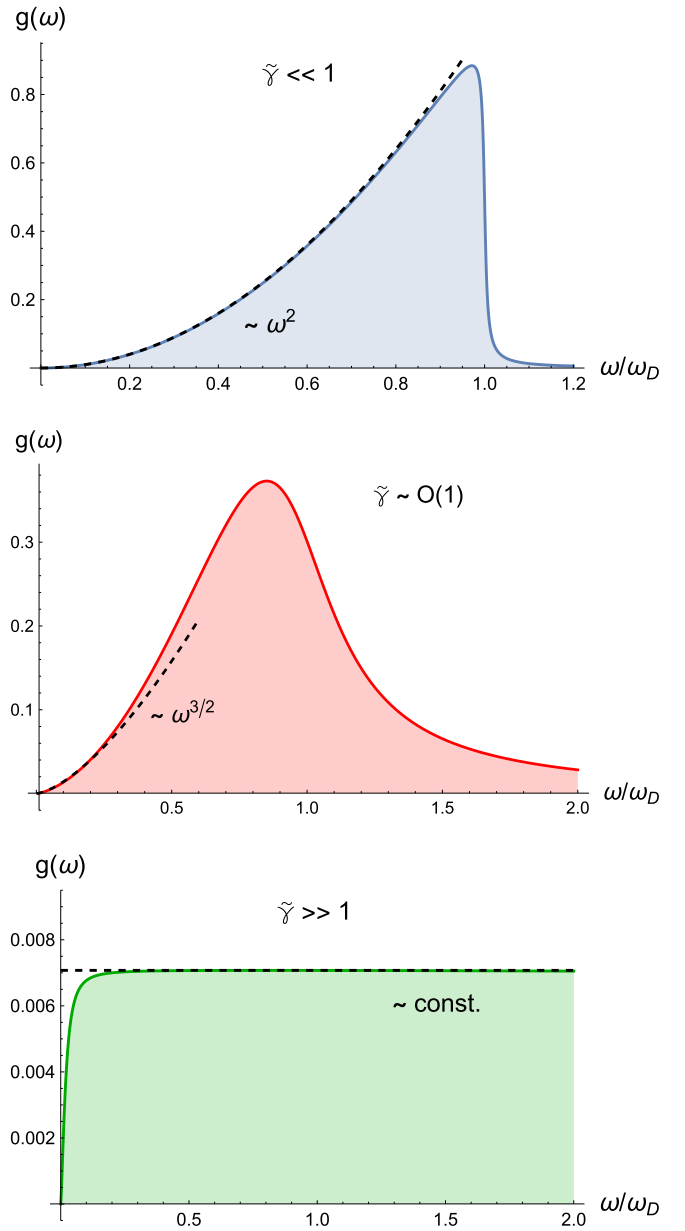


FIG. 4. Phason density of states in the three different regimes: $\tilde{\gamma} \ll 1$, $\tilde{\gamma} \sim O(1)$, and $\tilde{\gamma} \gg 1$. For simplicity, we set $k_D = v = 1$ and we set $\tilde{\gamma} = 10^{-2}$, 0.4, and 30 for the top, middle, and bottom panels, respectively.

Continuing with our analysis, the general trend of the heat capacity is shown in Fig. 5. The low-temperature scalings for different values of the phason damping are shown in Fig. 6, and they confirm the theoretical predictions.

Our results are compatible with the experimental data in Refs. [43,46], where a quasilinear scaling of the heat capacity is observed in incommensurate compounds. In the incommensurate dielectric $(\text{ClC}_6\text{H}_4)_2\text{SO}_2$ [43], a scaling $C(T) \propto T^{1.7}$ is reported. One could probably claim such a number to appear as a combination of our 5/2 and linear scalings. In the charge density compound charge-density-wave compound $\text{K}_{0.3}\text{MoO}_3$, a linear-in- T scaling is observed, as in our theoretical model in the overdamped limit. Finally, let us

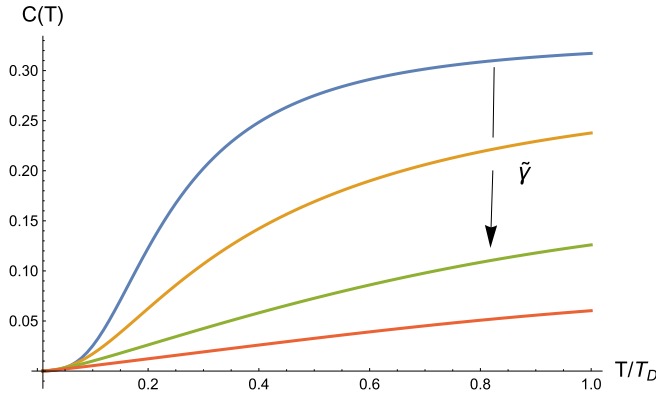


FIG. 5. Phason heat capacity as a function of the reduced temperature increasing the phason damping. Here, $v = 1$, $k_D = 1$, and $k_B = 1$; $\tilde{\gamma} = 0.001, 1, 4$, and 10 from top to bottom.

repeat that similar observations regarding a linear-in- T contribution from overdamped modes have already appeared in Refs. [35,36,43,45] using a slightly different formalism which includes a phason gap. Our results are in agreement with those presented there, where they overlap. Importantly, this indicates that overdamped bosonic modes would generally give a linear-in- T contribution to the heat capacity, independently of the details of their dispersion.

V. SUPERCONDUCTIVITY

In this section, we imagine the existence of a possible pairing channel between electrons and phasons, and we try to estimate how the hypothetical critical temperature would depend on the phason parameters. For simplicity, we will only consider an s -wave pairing. Additionally, we will neglect phonon-phason interactions and the more standard electron-phonon pairing channel.

We start by defining the Eliashberg function

$$\alpha^2 F(\mathbf{k}, \mathbf{k}', \omega) \equiv \mathcal{N}(\mu) |g_{\mathbf{k}, \mathbf{k}'}|^2 S(\omega, \mathbf{k} - \mathbf{k}'), \quad (23)$$

where we assume $\mathcal{N}(\mu)$ to be constant and $g_{\mathbf{k}, \mathbf{k}'}^2 = C(vq)^2$. This second assumption, which is valid for acoustic phonons

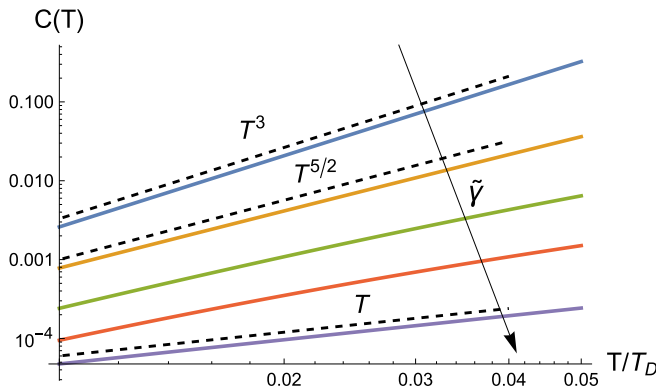


FIG. 6. Low-temperature scaling of the phason heat capacity increasing phason damping. Here, we set $k_D = k_B = v = 1$ and we set $\tilde{\gamma} = 0.001, 1, 4, 10$, and 1000 from top to bottom. Curves are shifted vertically for clarity.

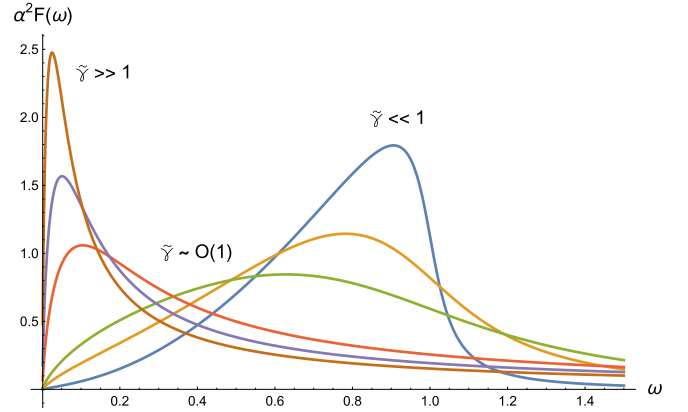


FIG. 7. The Eliashberg function $\alpha^2 F(\omega)$ as a function of the frequency upon increasing phason damping. Here, $v = k_D = 1$, $c_2 = 0.3$, and $k_F = 1/2$. $\tilde{\gamma} = 50, 10, 5, 1, 0.5$, and 0.1 from brown ($\tilde{\gamma} \gg 1$) to light blue ($\tilde{\gamma} \ll 1$).

[78,79], is the simplest possibility and hence the one chosen. After a few algebraic manipulations and averaging over the Fermi surface, we can rewrite the above expression as

$$\alpha^2 F(\omega) = c_2 \int_0^4 k_F^2 \xi S(\omega, k_F \sqrt{\xi}) d\xi, \quad (24)$$

where c_2 is a parameter to keep the normalized area $\int \alpha^2 F(\omega) d\omega = 1$ constant. This is equivalent to normalizing the phason spectral function as discussed in the previous sections. The integral can be calculated analytically, but the expression is rather cumbersome and therefore not shown. At low frequency, the Eliashberg function is linear in frequency:

$$\alpha^2 F(\omega) \sim \gamma \omega + \dots \quad (25)$$

Interestingly, this linear scaling is observed in amorphous superconductors [80] (see also Ref. [79]). We can prove that such a scaling is ubiquitous for overdamped bosonic modes with a damping term independent of frequency and wavevector, such as γ . The behavior of the normalized Eliashberg function is shown in Fig. 7 for different values of $\tilde{\gamma}$. The effective electron-phason coupling can be estimated as

$$\lambda = 2 \int_{-\infty}^{\infty} \frac{\alpha^2 F(\omega)}{\omega} d\omega. \quad (26)$$

Its dependence on the phason damping is shown in Fig. 8. It grows monotonically with the damping. This is just a consequence of the transfer of spectral weight to lower frequencies induced by the phason damping. This shows the possibility of achieving strongly coupled superconductivity as an effect of incommensurability and the consequent phason modes, in agreement with the experimental findings of Ref. [59]. Finally, using the simplified Allen-Dynes formula [81], we can estimate the corresponding critical temperature

$$T_c = \frac{\omega_{\log}}{1.2} \exp\left(-\frac{1.04(1+\lambda)}{\lambda - u^* - 0.62\lambda u^*}\right), \quad (27)$$

where ω_{\log} is the logarithmic average defined as

$$\omega_{\log} = \exp\left[\int_0^{\infty} \frac{2}{\lambda\omega} \alpha^2 F(\omega) \ln \omega d\omega\right]. \quad (28)$$

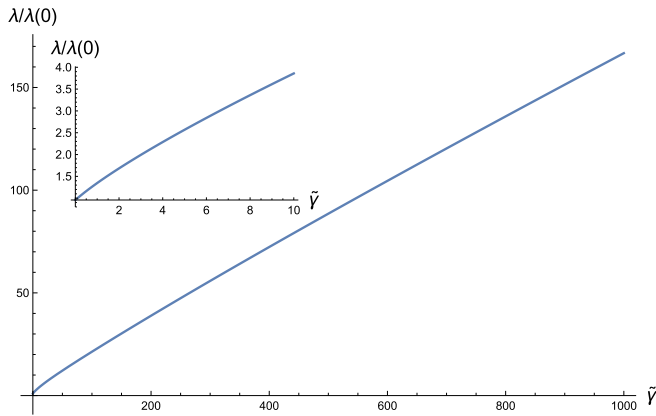


FIG. 8. The effective electron-phonon coupling λ as a function of the phason damping normalized by its value at zero damping. Here, $v = k_D = 1$, $c_2 = 0.3$, and $k_F = 1/2$. The inset zooms in on the smaller damping region.

T_c is shown as a function of the phason damping in Fig. 9. Interestingly, for small damping, the critical temperature grows up to a maximum critical value, after which the trend is inverted. The reason for this nonmonotonic behavior comes from the competition between the electron-phonon coupling λ and the average logarithmic frequency ω_{\log} . The first grows monotonically with the damping (see Fig. 8), while the second decreases with it, at least for large damping (see Fig. 10). Therefore T_c , as defined in Eq. (27), displays a nonmonotonic behavior. For small values of the damping, the effects of λ dominate and lead to an increase in T_c . For larger values of the damping, it is ω_{\log} which dominates and leads to a decrease in T_c . Interestingly, we find that this change of behavior happens for $\tilde{\gamma} \approx 1$. This seems to suggest that in the underdamped regime, the phason damping enhances the critical temperature, while in the overdamped regime its effect is opposite. This behavior is similar to that observed for spin glass phase in cuprates [82] and optical modes in Refs. [83,84], and it is expected to persist also in the limit of finite pinning frequency, $\omega_0 \neq 0$.

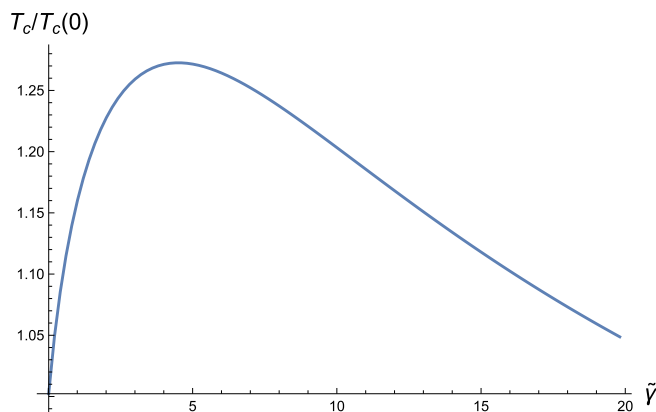


FIG. 9. The superconducting critical temperature T_c as a function of the phason damping. Here, $v = k_D = 1$, $c_2 = 0.3$, $k_F = 1/2$, and $\mu^* = 0.1$.

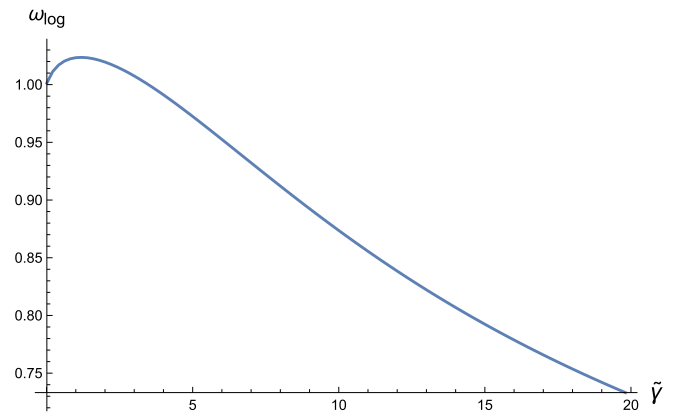


FIG. 10. The average ω_{\log} as a function of the phason damping. Here, $v = k_D = 1$, $c_2 = 0.3$, and $k_F = 1/2$.

Let us discuss our results in comparison to the existing literature. First, the strong enhancement of the effective coupling visible in Fig. 9 is compatible with the experimental observations in Ref. [59], where the strongly coupled nature of superconductivity has been ascribed to the phason mode and its redshifted spectral weight, as a consequence of its overdamped nature. Second, recent theoretical analysis [60] has shown that incommensurability can provide an enhancement of the superconducting critical temperature, but only in the regime of weak or intermediate coupling. Our findings offer a different but compatible interpretation of the same fact. Phasons, and in particular phason damping, enhance the critical temperature T_c only in the regime of small damping (i.e., the underdamped regime), in which the Eliashberg coupling is not too large (see Fig. 9), as advocated in Ref. [60].

VI. DISCUSSION AND CONCLUSIONS

In this paper, we have studied in detail the effects of phason modes on the vibrational, thermodynamic, and superconducting properties of incommensurate structures. For simplicity, we have worked in the limit in which the phason pinning frequency is negligible compared with its damping. Our analysis revealed several interesting features which appear, at least qualitatively, compatible with the existing experimental data and other theoretical studies in the literature.

We have confirmed that overdamped phasons, or, more generally, overdamped excitations, induce glassylike features in the heat capacity and, in particular, a pronounced linear-in- T contribution, which is proportional to their diffusive constant and more evident in the limit of very large damping. We have also found an intermediate scaling regime, which combined with the linear scaling emerging at large damping, could explain the quasilinear behaviors observed experimentally in certain incommensurate compounds [43,46]. Interestingly, our results not only confirm the previous theoretical studies in Refs. [34–36] but also suggest a different scaling of the linear-in- T contribution with the phason damping. The discrepancy is due to the different limits taken. In particular, we assume from the start that the pinning frequency is negligible, while the works referred to above do not. It would be interesting to investigate this point further.

Moreover, inspired by the results in Refs. [57,58], we have investigated a hypothetical phason-induced superconductivity using the Eliashberg formalism and treating naively the phasons as if they were standard phonons. Despite the simplicity of our assumptions, which certainly necessitate further validation in the near future, we have been able to extract several interesting features which appear to be in agreement with recent observations. First, we have shown that, because of the overdamped nature of phasons (which is usually not the case for phonons, unless in situations with very strong anharmonicity), the effective coupling can be strongly enhanced, leading to strongly coupled superconductivity. Similar results, and experimental verifications, have been presented in Ref. [59] for the quasiperiodic host-guest structure of elemental bismuth at high pressure, Bi-III. Additionally, we have predicted a nonmonotonic behavior of the superconducting critical temperature T_c as a function of the phason damping. The maximum in T_c appears approximately at the underdamped-to-overdamped-crossover scale, indicating that only underdamped phasons contribute positively to superconductivity. Qualitatively, this finding is in agreement with the recent results in Ref. [60], since the underdamped regime corresponds to the range of weak or intermediate effective coupling λ . This observation deserves further studies.

We foresee several improvements to our setup and arguments against its simplicity. As a concrete example, we have been completely agnostic about the microscopic details of a possible phason-electron coupling, and even about the possibility that the latter exists. Preliminary studies of the phason-electron coupling in twisted bilayer graphene have appeared in Refs. [22,57,58] and suggested that at least for such a scenario the pairing mechanism might be more complicated than what we have modeled (e.g., dependent on the twist angle θ , etc.). Additionally, we have ignored the effects of phonon-phason interactions and the fact that the dispersion relation of moiré phonons and their coupling to electrons could also be strongly modified.

On the other hand, it is important to identify some experimentally detectable distinctions between phonon-mediated and phason-mediated superconductivity. Searching for violations of the isotope effect is a viable option. As shown in the previous section, the pairing ability of the phason is maximal for values of the damping of $O(1)$. In the presence of such large friction, the long-wavelength phason is not a propagating mode, like the vibrations of a harmonic lattice, but is rather a diffusivelike overdamped excitation. Therefore we do not expect its frequency to have a simple relation, or even any relation, with the atomic mass. This would immediately imply the violation or absence of the isotope effect in phason-mediated superconductivity, which is testable in the laboratory.

Despite the simplicity of our analysis, and the bold assumptions, we believe that this might constitute a baby step towards a deeper understanding of phason properties and their effects on thermodynamics, transport, and superconductivity, which are potentially relevant for a large class of quantum materials, joined under the umbrella of incommensurate structures. We expect more and more signatures of these overdamped modes to appear in the near future. It would be important to think about possible measurable effects arising

from the presence of an overdamped phason mode. The analysis of the diffusive dynamics of charge order might be a good place to start [85,86]. It is also important to think about a possible universality regarding the emergence of glassy properties from overdamped and soft bosonic modes. This could bring together apparently different scenarios such as amorphous systems, incommensurate structures, strange metals, thermoelectrics or materials with rattling modes, and systems exhibiting giant anharmonicity.

Finally, in the context of twisted bilayer graphene or other two-dimensional (2D) heterostructures, it would be interesting to understand whether phasons could mediate the formation of polarons or excitons and drive the emergence of the strongly insulating states in 2D bilayer systems.

ACKNOWLEDGMENTS

We thank Hector Ochoa for useful comments and suggestions on a preliminary version of this manuscript. We would like to thank Friedrich Malte Grosche for telling us about Ref. [87] and for pointing out to us the existence of 1D-like phason modes in certain compounds. We would like to thank Michael Schmiedeberg for clarifications about the nature of the phason. We would like to thank Matteo Mitrano for discussions about the possible experimental consequences of an overdamped phason. We thank S. Nakamura, J. Douglas, Y. Wang, and M. Landry for several discussions about phasons and their existence. We thank G. Ghiringhelli, R. Arpaia, M. Grosche, S. Mandyam, Y. Ishii, and J. Ma for useful discussions about superconductivity and incommensurate structures. C.J. and M.B. acknowledge the support of the Shanghai Municipal Science and Technology Major Project (Grant No. 2019SHZDZX01) and the sponsorship from the Yangyang Development Fund. A.Z. gratefully acknowledges funding from the European Union through Horizon Europe ERC Grant No. 101043968 “Multimech” and from the U.S. Army Research Office through Contract No. W911NF-22-2-0256.

APPENDIX A: COMPARISON WITH THE HEAT CAPACITY OF A DAMPED HARMONIC OSCILLATOR

In 1987, Pippard computed the entropy of a damped harmonic oscillator using an analogy with the physics of RLC circuits [87]. The final result of such an analysis, based on classical physics, is that the entropy of a damped harmonic oscillator is given by

$$S = \frac{k_B Q}{\pi} \int_0^\infty \frac{(x^2 + 1)[\beta x \coth(\beta x) - \ln(2 \sinh(\beta x))]}{x^2 + Q^2(x^2 - 1)^2} dx, \quad (\text{A1})$$

where $\beta = \bar{\omega}/2k_B T$ (with $\bar{\omega}$ being the characteristic frequency of the harmonic oscillator), and Q is the quality factor $Q = \bar{\omega}/\gamma$, where γ is the damping parameter. In particular, by decreasing the value of Q , the harmonic oscillator passes from being underdamped to overdamped. Using the above expression for the entropy, one can compute the heat capacity using

$$C(T) = T \frac{\partial S}{\partial T}. \quad (\text{A2})$$

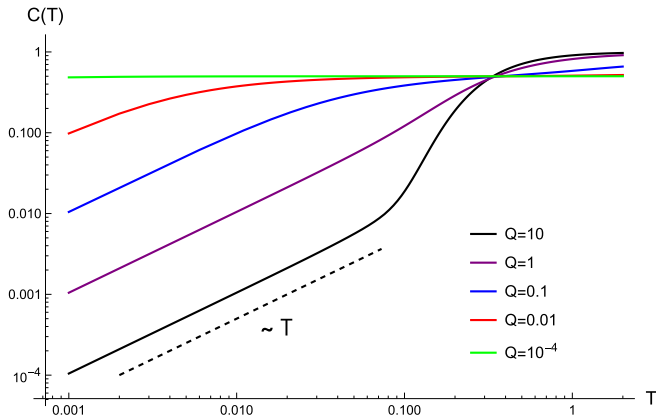


FIG. 11. The heat capacity of a damped harmonic oscillator obtained from Pippard's analysis [87] for different values of the parameter Q . For simplicity, here $k_b = \bar{\omega} = 1$. The dashed line indicates the linear-in- T scaling.

The results of this simple computation are shown in Fig. 11, where the heat capacity as a function of temperature is plotted for different values of the parameter Q . Interestingly, we observe a clear linear-in- T regime at low temperature. The range in which this scaling appears becomes smaller by decreasing Q . This is compatible, at least qualitatively, with our results, in which an overdamped phason also gives rise to a linear-in- T contribution to the heat capacity. It would be interesting to explore further the relation between our results and Pippard's computations [87]. Notice that our computation relies on the quantum bosonic nature of the phason excitations at low temperature, while Pippard's analysis is purely classical. Interestingly, a linear-in- T heat capacity has been obtained as well for a damped quantum oscillator in Ref. [88]. This strongly hints towards the universality of this behavior in the context of overdamped modes.

APPENDIX B: OVERDAMPED PHASON WITH RESTRICTED MOBILITY

In high-pressure bismuth [59] and other host-guest structures, the phason dispersion appears to be 1D-like with a strong dispersion along the chains but flat dispersion perpendicular to the chains. Therefore, in this Appendix, we find it interesting to repeat our computation by considering an overdamped phason mode which propagates only in some of the three spatial directions. This amounts to modifying the equation for the density of states as

$$g(\omega) \propto \int_0^{k_D} \frac{\gamma \omega}{(\omega^2 - \omega_0^2 - v^2 k^2)^2 + \gamma^2 \omega^2} k^n dk, \quad (\text{B1})$$

where $n = 0, 1$, and 2 correspond to 1D, 2D, and 3D propagating phasons, respectively, and we have added a bare energy ω_0 to take into account the flat dispersion in the other directions. By analytically expanding the above expression in the overdamped regime, defined as γ being much larger than every other frequency scale, we obtain that the vibrational density of states at low frequency is constant, and indeed proportional to $1/\gamma$, independently of n . That is to say that, independently of the 1D, 2D, or 3D nature of the overdamped phason, in such a regime, the overdamped phason will always contribute to the heat capacity with a linear-in- T term, which is in principle observable in experiments. Let us also emphasize that in the overdamped limit, $\gamma \gg \omega_0$ and therefore an optical-like and a propagating phason would give exactly the same result. This is compatible with the results obtained in the main text and the comparison with those of Ref. [35], where a bare energy (or pinning frequency) ω_0 for the phason is considered. The main difference in the presence of a finite ω_0 is the appearance of a boson-peak-like feature at larger energies (see Ref. [35] for details). If we insist on ignoring the energy gap ω_0 and we set it to zero from the start, then for intermediate values of the damping coefficient we find that $g(\omega) \propto \omega^{(n+1)/2}$ and $C(T) \propto T^{(n+1)/2+1}$, where $n+1$ is the number of spatial directions along which the phason propagates.

-
- [1] P. M. Chaikin and T. C. Lubensky, *Principles of Condensed Matter Physics* (Cambridge University Press, Cambridge, 1995).
- [2] H. Leutwyler, *Helv. Phys. Acta* **70**, 275 (1997).
- [3] In this paper, we will not consider optical modes. Therefore, when we mention phonons, we will always refer to acoustic ones.
- [4] M. Baggioli and B. Goutéraux, *Rev. Mod. Phys.* **95**, 011001 (2023).
- [5] C. Kittel, *Introduction to Solid State Physics*, 8th ed. (Wiley, New York, 2021).
- [6] J. Ziman, *Electrons and Phonons: The Theory of Transport Phenomena in Solids*, International Series of Monographs on Physics (Oxford University Press, Oxford, 2001).
- [7] J. P. Carbotte and F. Marsiglio, in *The Physics of Superconductors: Vol. I. Conventional and High- T_c Superconductors*, edited by K. H. Bennemann and J. B. Ketterson (Springer, Berlin, 2003), pp. 233–345.
- [8] B. D. E. McNiven, J. P. F. LeBlanc, and G. T. Andrews, *Phys. Rev. B* **106**, 054113 (2022).
- [9] I. Loa, L. F. Lundegaard, M. I. McMahon, S. R. Evans, A. Bossak, and M. Krisch, *Phys. Rev. Lett.* **99**, 035501 (2007).
- [10] R. Blinc, V. Rutar, J. Dolinsek, B. Topič, F. Milia, and S. Žumer, *Ferroelectrics* **66**, 57 (1986).
- [11] C. M. Zeyen, *Phys. B+C (Amsterdam)* **120**, 283 (1983).
- [12] M. Quilichini and R. Currat, *Solid State Commun.* **48**, 1011 (1983).
- [13] J. Etrillard, Ph. Bourges, H. F. He, B. Keimer, B. Liang, and C. T. Lin, *Europhys. Lett.* **55**, 201 (2001).
- [14] M. D. Boissieu, *Philos. Mag.* **88**, 2295 (2008).
- [15] M. de Boissieu, *Isr. J. Chem.* **51**, 1292 (2011).
- [16] M. Widom, *Philos. Mag.* **88**, 2339 (2008).
- [17] R. Currat and T. Janssen, *Solid State Phys.* **41**, 201 (1988).
- [18] J. A. Kromer, M. Schmiedeberg, J. Roth, and H. Stark, *Phys. Rev. Lett.* **108**, 218301 (2012).

- [19] J. P. Pouget, G. Shirane, J. M. Hastings, A. J. Heeger, N. D. Miro, and A. G. MacDiarmid, *Phys. Rev. B* **18**, 3645 (1978).
- [20] J. M. Hastings, J. P. Pouget, G. Shirane, A. J. Heeger, N. D. Miro, and A. G. MacDiarmid, *Phys. Rev. Lett.* **39**, 1484 (1977).
- [21] G. Grüner, *Rev. Mod. Phys.* **60**, 1129 (1988).
- [22] H. Ochoa and R. M. Fernandes, *Phys. Rev. Lett.* **128**, 065901 (2022).
- [23] T. C. Lubensky, S. Ramaswamy, and J. Toner, *Phys. Rev. B* **32**, 7444 (1985).
- [24] R. Currat, E. Kats, and I. Luk'yanchuk, *Eur. Phys. J. B* **26**, 339 (2002).
- [25] M. Baggioli and M. Landry, *SciPost Phys.* **9**, 062 (2020).
- [26] M. Baggioli, M. Vasin, V. Brazhkin, and K. Trachenko, *Phys. Rep.* **865**, 1 (2020).
- [27] S. Grozdanov, A. Lucas, and N. Poovuttikul, *Phys. Rev. D* **99**, 086012 (2019).
- [28] W. Finger and T. M. Rice, *Phys. Rev. Lett.* **49**, 468 (1982).
- [29] R. Zeyher and W. Finger, *Phys. Rev. Lett.* **49**, 1833 (1982).
- [30] W. Finger and T. M. Rice, *Phys. Rev. B* **28**, 340 (1983).
- [31] J. D. Axe and P. Bak, *Phys. Rev. B* **26**, 4963 (1982).
- [32] H. Cailleau, F. Moussa, C. Zeyen, and J. Bouillot, *Solid State Commun.* **33**, 407 (1980).
- [33] K. B. Lyons, R. N. Bhatt, T. J. Negran, and H. J. Guggenheim, *Phys. Rev. B* **25**, 1791 (1982).
- [34] R. Bag, S. Hazra, R. N. Kini, and S. Singh, *Phys. Rev. B* **99**, 054305 (2019).
- [35] A. Cano and A. P. Levanyuk, *Phys. Rev. Lett.* **93**, 245902 (2004).
- [36] G. Reményi, S. Sahling, K. Biljaković, D. Starešinić, J.-C. Lasjaunias, J. E. Lorenzo, P. Monceau, and A. Cano, *Phys. Rev. Lett.* **114**, 195502 (2015).
- [37] M. A. Ramos, *Low-Temperature Thermal and Vibrational Properties of Disordered Solids* (World Scientific, Singapore, 2022).
- [38] J. M. Schliesser and B. F. Woodfield, *J. Phys.: Condens. Matter* **27**, 285402 (2015).
- [39] M. Baggioli and A. Zaccone, *J. Phys. Mater.* **3**, 015004 (2020).
- [40] T. Takabatake, K. Suekuni, T. Nakayama, and E. Kaneshita, *Rev. Mod. Phys.* **86**, 669 (2014).
- [41] M. Moratalla, J. F. Gebbia, M. A. Ramos, L. C. Pardo, S. Mukhopadhyay, S. Rudić, F. Fernandez-Alonso, F. J. Bermejo, and J. L. Tamarit, *Phys. Rev. B* **99**, 024301 (2019).
- [42] A. I. Krivchikov, A. Jeżowski, D. Szewczyk, O. A. Korolyuk, O. O. Romantsova, L. M. Buravtseva, C. Cazorla, and J. L. Tamarit, *J. Phys. Chem. Lett.* **13**, 5061 (2022).
- [43] J. Etrillard, J. C. Lasjaunias, K. Biljakovic, B. Toudic, and G. Coddens, *Phys. Rev. Lett.* **76**, 2334 (1996).
- [44] M. Baggioli and A. Zaccone, *Phys. Rev. Res.* **1**, 012010(R) (2019).
- [45] M. Baggioli and A. Zaccone, *Int. J. Mod. Phys. B* **35**, 2130002 (2021).
- [46] K. J. Dahlhauser, A. C. Anderson, and G. Mozurkewich, *Phys. Rev. B* **34**, 4432 (1986).
- [47] J. Odin, J. C. Lasjaunias, K. Biljaković, K. Hasselbach, and P. Monceau, *Eur. Phys. J. B* **24**, 315 (2001).
- [48] We thank Hector Ochoa for pointing this out to us.
- [49] L. N. Bulaevskii and M. P. Maley, *Phys. Rev. Lett.* **71**, 3541 (1993).
- [50] G. Blatter and B. I. Ivlev, *Phys. Rev. B* **50**, 10272 (1994).
- [51] R. Iengo and C. A. Scrucca, *Phys. Rev. B* **57**, 6046 (1998).
- [52] A. Erzan, E. Veermans, R. Heijungs, and L. Pietronero, *Phys. Rev. B* **41**, 11522 (1990).
- [53] P. B. Littlewood and R. Rammal, *Phys. Rev. B* **38**, 2675 (1988).
- [54] M. Koshino and Y.-W. Son, *Phys. Rev. B* **100**, 075416 (2019).
- [55] I. Maity, M. H. Naik, P. K. Maiti, H. R. Krishnamurthy, and M. Jain, *Phys. Rev. Res.* **2**, 013335 (2020).
- [56] Q. Gao and E. Khalaf, *Phys. Rev. B* **106**, 075420 (2022).
- [57] H. Ochoa, *Phys. Rev. B* **100**, 155426 (2019).
- [58] H. Ochoa and R. M. Fernandes, [arXiv:2302.00043](https://arxiv.org/abs/2302.00043).
- [59] P. Brown, K. Semeniuk, D. Wang, B. Monserrat, C. J. Pickard, and F. M. Grosche, *Sci. Adv.* **4**, eaao4793 (2018).
- [60] R. Oliveira, M. Gonçalves, P. Ribeiro, E. V. Castro, and B. Amorim, [arXiv:2303.17656](https://arxiv.org/abs/2303.17656).
- [61] J. Whaley-Baldwin, M. Hutcheon, and C. J. Pickard, *Phys. Rev. B* **103**, 214111 (2021).
- [62] S.-c. Zhu, Z.-b. Huang, Q. Hu, and L. Xu, *Phys. Chem. Chem. Phys.* **24**, 7007 (2022).
- [63] K. Kamiya, T. Takeuchi, N. Kabeya, N. Wada, T. Ishimasa, A. Ochiai, K. Deguchi, K. Imura, and N. K. Sato, *Nat. Commun.* **9**, 154 (2018).
- [64] D. H. Torchinsky, F. Mahmood, A. T. Bollinger, I. Božović, and N. Gedik, *Nat. Mater.* **12**, 387 (2013).
- [65] S. Sugai, Y. Takayanagi, and N. Hayamizu, *Phys. Rev. Lett.* **96**, 137003 (2006).
- [66] R. Arpaia, L. Martinelli, M. M. Sala, S. Caprara, A. Nag, N. B. Brookes, P. Camisa, Q. Li, Q. Gao, X. Zhou, M. Garcia-Fernandez, K.-J. Zhou, E. Schierle, T. Bauch, Y. Y. Peng, C. Di Castro, M. Grilli, F. Lombardi, L. Braicovich, and G. Ghiringhelli, [arXiv:2208.13918](https://arxiv.org/abs/2208.13918).
- [67] E. Bertel and A. Menzel, *Symmetry* **8**, 45 (2016).
- [68] M. Grilli, C. Di Castro, G. Mirarchi, G. Seibold, and S. Caprara, *Symmetry* **15**, 569 (2023).
- [69] S. Caprara, C. D. Castro, G. Mirarchi, G. Seibold, and M. Grilli, *Commun. Phys.* **5**, 10 (2022).
- [70] G. Seibold, R. Arpaia, Y. Y. Peng, R. Fumagalli, L. Braicovich, C. Di Castro, M. Grilli, G. C. Ghiringhelli, and S. Caprara, *Commun. Phys.* **4**, 7 (2021).
- [71] R. Arpaia, S. Caprara, R. Fumagalli, G. De Vecchi, Y. Peng, E. Andersson, D. Betto, G. De Luca, N. Brookes, F. Lombardi, M. Salluzzo, L. Braicovich, C. Di Castro, M. Grilli, and G. Ghiringhelli, *Science* **365**, 906 (2019).
- [72] J. Etrillard, L. Bourgeois, P. Bourges, B. Liang, C. T. Lin, and B. Keimer, *Europhys. Lett.* **66**, 246 (2004).
- [73] B. D. E. McNiven, J. P. F. LeBlanc, and G. T. Andrews, *Mater. Res. Express* **10**, 026001 (2023).
- [74] T. Mitchell and A. Misra, *Mater. Sci. Eng.: A* **261**, 106 (1999).
- [75] S. Carr, D. Massatt, S. B. Torrisi, P. Cazeaux, M. Luskin, and E. Kaxiras, *Phys. Rev. B* **98**, 224102 (2018).
- [76] C. Setty, M. Baggioli, and A. Zaccone, [arXiv:2303.12977](https://arxiv.org/abs/2303.12977).
- [77] J. Hansen and I. McDonald, *Theory of Simple Liquids: With Applications to Soft Matter* (Elsevier Science, New York, 2013).
- [78] S. Engelsberg and J. R. Schrieffer, *Phys. Rev.* **131**, 993 (1963).
- [79] G. Bergmann, *Phys. Rev. B* **3**, 3797 (1971).
- [80] B. Keck and A. Schmid, *J. Low Temp. Phys.* **24**, 611 (1976).
- [81] P. B. Allen and R. C. Dynes, *Phys. Rev. B* **12**, 905 (1975).
- [82] C. Setty, *Phys. Rev. B* **99**, 144523 (2019).
- [83] C. Setty, M. Baggioli, and A. Zaccone, *Phys. Rev. B* **102**, 174506 (2020).

- [84] C. Jiang, E. Beneduce, M. Baggioli, C. Setty, and A. Zaccane, *J. Phys.: Condens. Matter* **35**, 164003 (2023).
- [85] M. Mitrano, S. Lee, A. A. Husain, M. Zhu, G. de la Peña Muñoz, S. X.-L. Sun, Y. I. Joe, A. H. Reid, S. F. Wandel, G. Coslovich, W. Schlotter, T. van Driel, J. Schneeloch, G. D. Gu, N. Goldenfeld, and P. Abbamonte, *Phys. Rev. B* **100**, 205125 (2019).
- [86] M. Mitrano, S. Lee, A. A. Husain, L. Delacretaz, M. Zhu, G. de la Peña Muñoz, S. X.-L. Sun, Y. I. Joe, A. H. Reid, S. F. Wandel, G. Coslovich, W. Schlotter, T. van Driel, J. Schneeloch, G. D. Gu, S. Hartnoll, N. Goldenfeld, and P. Abbamonte, *Sci. Adv.* **5**, eaax3346 (2019).
- [87] A. B. Pippard, *Eur. J. Phys.* **8**, 55 (1987).
- [88] G.-L. Ingold, P. Hänggi, and P. Talkner, *Phys. Rev. E* **79**, 061105 (2009).